

Figure S1. Graded expression of Dmrt3 and Dmrta2 in the developing cerebral cortex of mice.

A, Schematic illustration of the domain structure of mouse Dmrt proteins. The three Dmrt proteins (Dmrt3, Dmrt1, and Dmrta2) are subcategorized as Dmrt “A” family proteins due to their conserved DMA domain. **B**, Molecular phylogenetic tree for the DM domains of ten mouse Dmrt proteins, the *Drosophila* double sex (dsx) protein, and the *C. elegans* mab-3 protein. **C**, Relative gene expression of *Dmrt* genes in the dorsal telencephalon at E14.5, as analyzed by deep sequencing. The values are represented as relative value to the *Dmrta2* expression. **D**, Whole-mount immunofluorescence for Dmrt3 and Dmrta2 in E9.5 mouse embryos. Scale bars, 1 mm. **E**, Immunofluorescence for Dmrt3 and Dmrta2 in coronal sections of the mouse telencephalon at E12.5. Scale bars, 50 μ m. **F**, Schematic showing four subdivided areas of the dorsal telencephalon for which gene expression was examined as in (G). AL, anterior-lateral; AM, anterior-medial; PL, posterior-lateral; PM, posterior-medial. **G**, Expression of *Dmrt3*, *Dmrta2*, and marker genes expressed in a gradient in the developing telencephalon. Expression is normalized against *Sox2*, as analyzed by qPCR in the four brain regions indicated in (F). The error bars represent \pm s.d. ($n=4$ per group). **H**, Schematic summarizing the graded expression of Dmrt3 and Dmrta2 in the developing mouse dorsal telencephalon. **I**, Lateral views (left) and top views of the forebrain (right) of E15.5 wild-type and *Dmrt3/Dmrta2* double heterozygous embryos. **J**, Immunofluorescence for Gad2, Tbr1, and Pou3f2 in coronal sections of the telencephalon in the wild-type and *Dmrt3/Dmrta2* double heterozygous E15.5 embryos. **K**, Immunofluorescence for Pax6 and Gsx2 in coronal sections of the telencephalon of wild-type and *Dmrt3/Dmrta2* double heterozygous E12.5 embryos. **L**, Immunofluorescence for Sp8 and Isl1 in coronal sections of the telencephalon of wild-type and *Dmrt3/Dmrta2* double heterozygous E12.5 embryos. In (K) and (L), the right panels represent higher magnifications of the boxed regions indicated in the left panels.

D, dorsal; L, lateral; A, anterior; V, ventricle; LGE, lateral ganglionic eminence; MGE, medial ganglionic eminence. In all immunofluorescence images, the yellow dotted lines indicate the ventricular surface. Scale bars, 100 μ m.

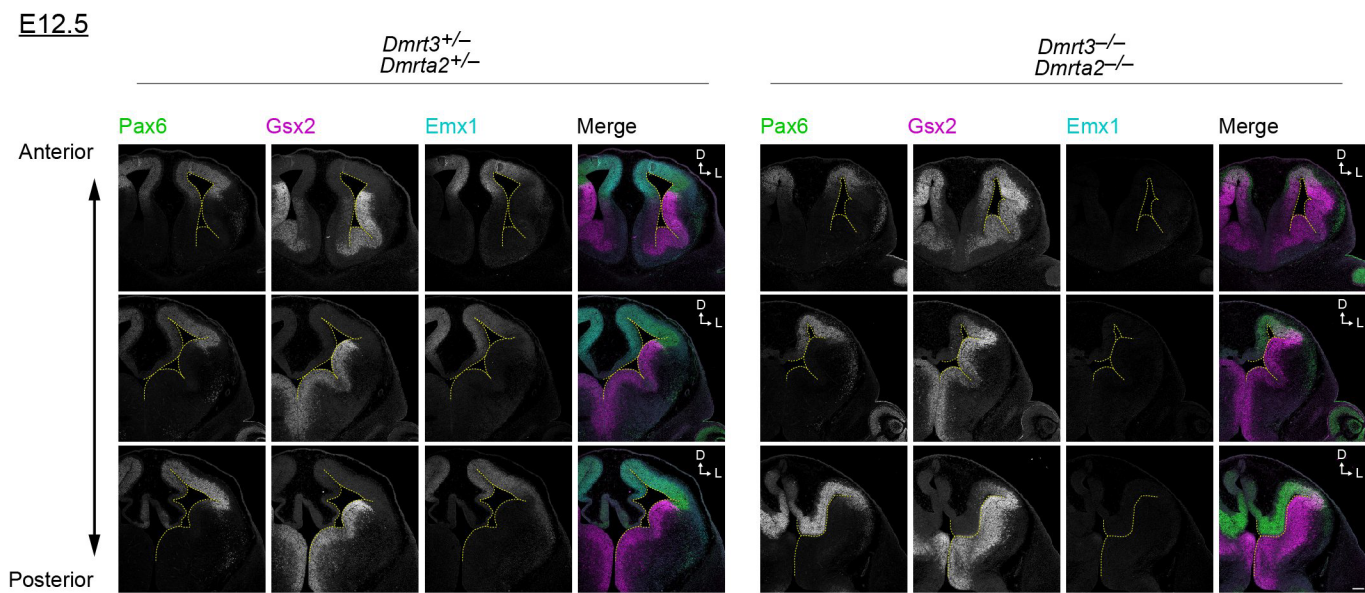
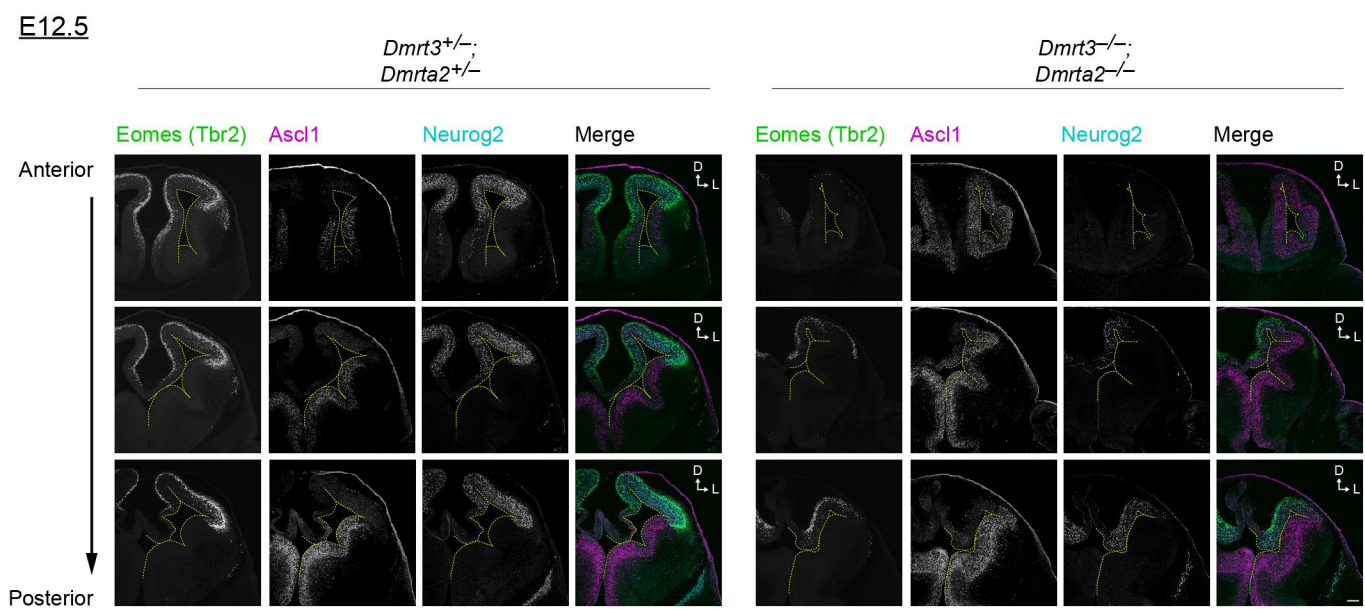
A**B**

Figure S2. Aberrant expression of transcription factors involved in cerebral cortical development.

A, B, Immunofluorescence for Pax6, Gsx2, and Emx1 (A), or Ascl1, Eomes (Tbr2), and Neurog2 (B), in coronal sections across the anteroposterior telencephalon of *Dmrt3/Dmrt2* mutant E12.5 embryos. The images are aligned along the anteroposterior axis from top to bottom. The dotted lines indicate the ventricular surface. Scale bars, 100 μ m.

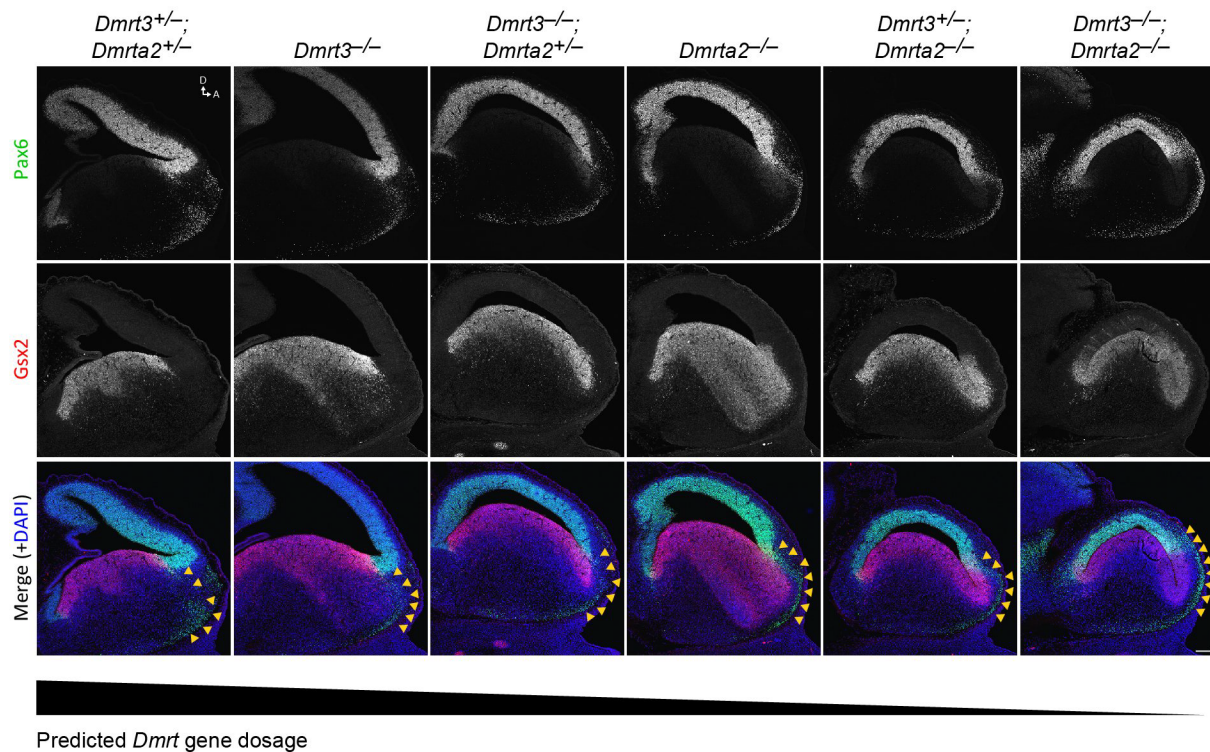
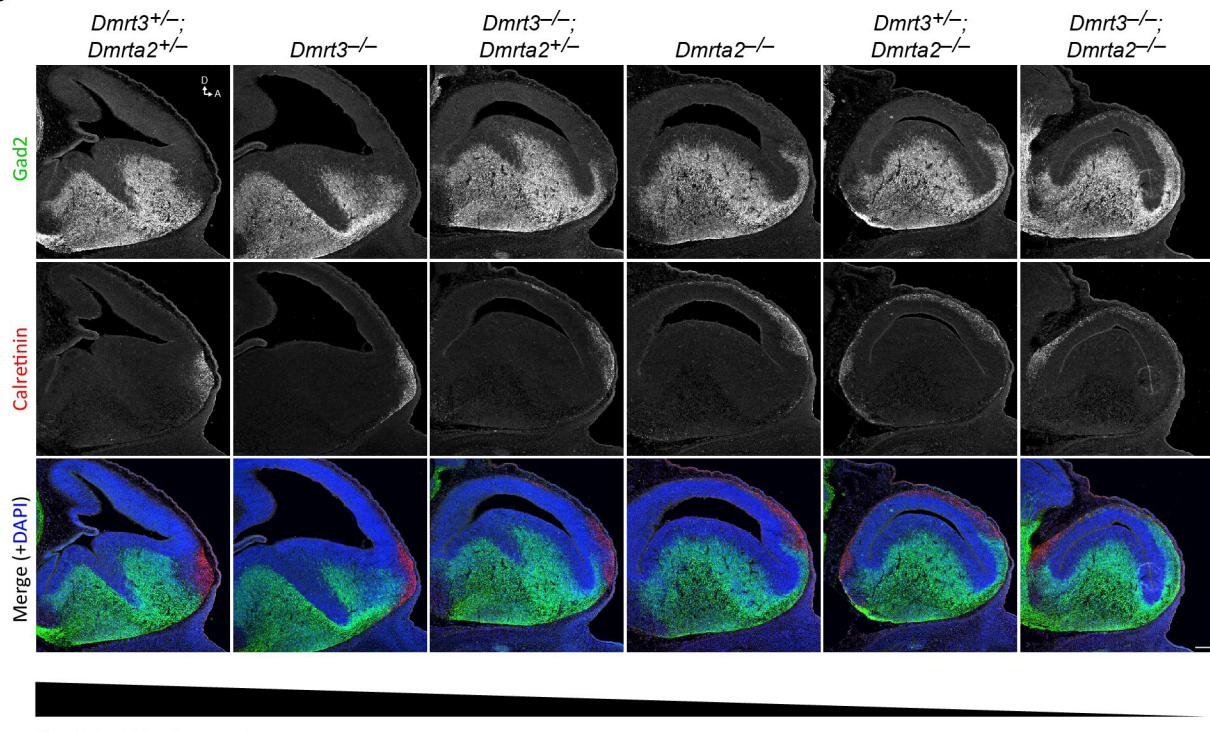
APredicted *Dmrt* gene dosage**B**Predicted *Dmrt* gene dosage

Figure S3. Gene dosage-dependent suppression of GABAergic neuron production and the expression of Gsx2 by *Dmrt* factors.

A, B, Immunofluorescence for Pax6 and Gsx2 (A), or Gad2 and Calretinin (B), in sagittal sections of the telencephalon of E12.5 *Dmrt* mutant embryos. The yellow arrowheads in (A) indicate the pax6-positive-migrating olfactory bulb interneurons. Scale bars, 100 μ m.

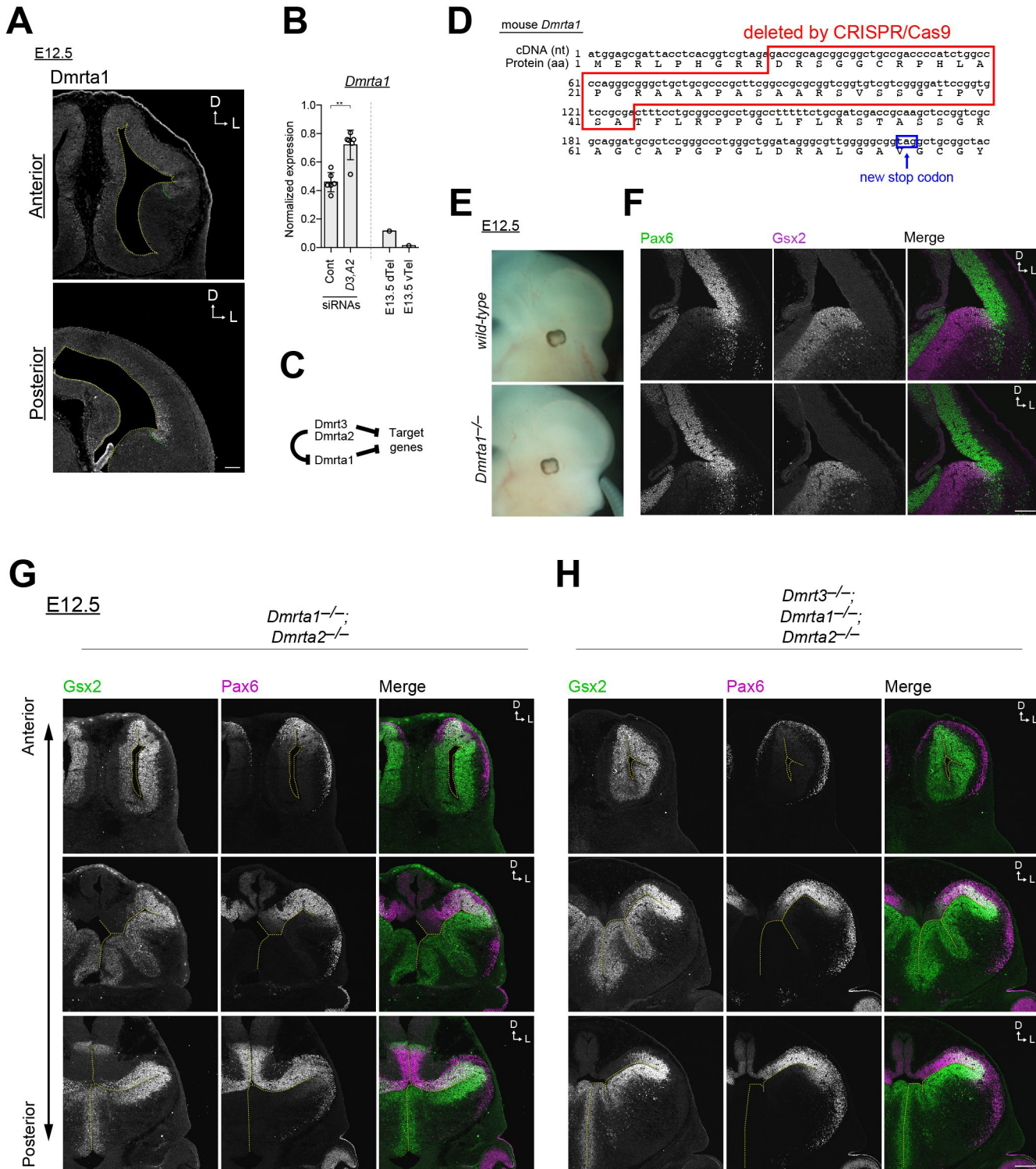


Figure S4. Double or triple mutants for *Dmrt* genes, including *Dmrtal*, phenocopies mutants for *Dmrt3* and *Dmrt2*.

A, *Dmrtal* immunofluorescence in coronal sections from the anterior and posterior E12.5 mouse telencephalon. **B**, Gene expression of *Dmrtal* normalized to *Sox2* as analyzed by qPCR in cells electroporated with control siRNAs those targeting *Dmrt3* and *Dmrt2*. The error bars represent \pm s.d. ($n=6$ per group). The statistical significance was determined using Student's *t*-test with Welch's correction (** $p<0.01$). **C**, The possible regulatory mechanism for *Dmrtal* expression. **D**, Confirmation of successful CRISPR/Cas9-mediated deletion of the genomic sequence around the *Dmrtal* start codon in ES cells. These ES cells were used to generate *Dmrtal* knockout mutant mice. **E**, Lateral views of the head of E12.5 *Dmrtal* mutant embryos. **F**, **G**, **H**, Immunofluorescence for Pax6 and Gsx2 in coronal sections across the anteroposterior telencephalon of E12.5 *Dmrtal* single mutant (F), *Dmrt3/Dmrt2* double mutant (G), and *Dmrt3/Dmrt2/Dmrtal* triple mutant (H) embryos. The images are aligned along the anteroposterior axis from top to bottom. The dotted lines indicate the ventricular surface. Scale bars, 100 μ m.

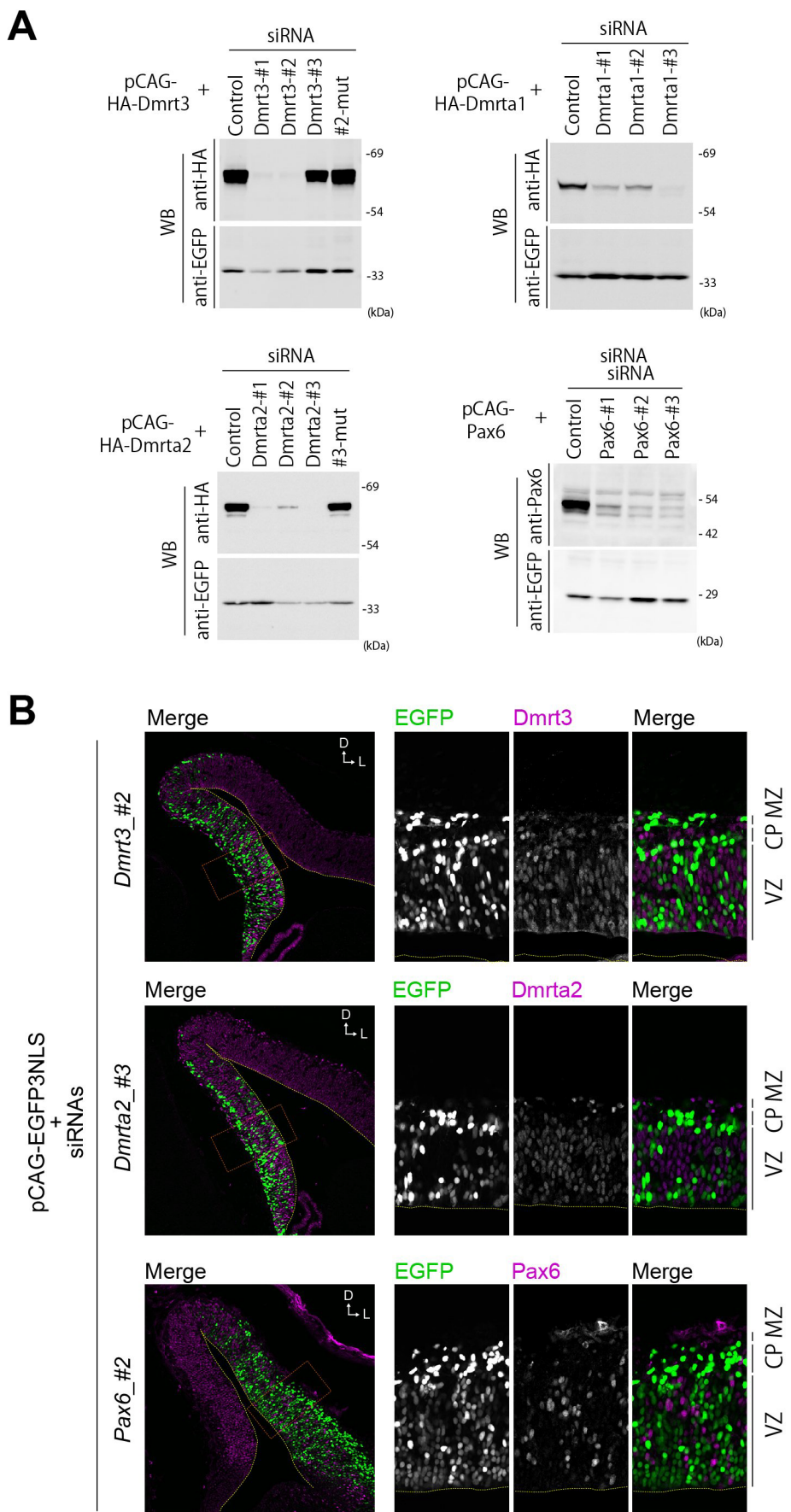


Figure S5. Efficient knockdown of target genes in the developing cerebral cortex via *in utero* electroporation of siRNAs.

A, Evaluation of the knockdown efficiency of siRNAs against indicated *Dmrt* genes or Pax6 by western blotting using HEK293 cells. **B**, Confirmation of an effective knockdown of endogenous protein expression via siRNA transfection into neural progenitors using *in utero* electroporation. Immunofluorescence was performed for *Dmr3*, *Dmrt2*, and Pax6 in brains electroporated with siRNAs targeting *Dmrt3*, *Dmrt2*, and *Pax6*, respectively. Right panels represent higher magnifications of the boxed regions indicated in the left panels.

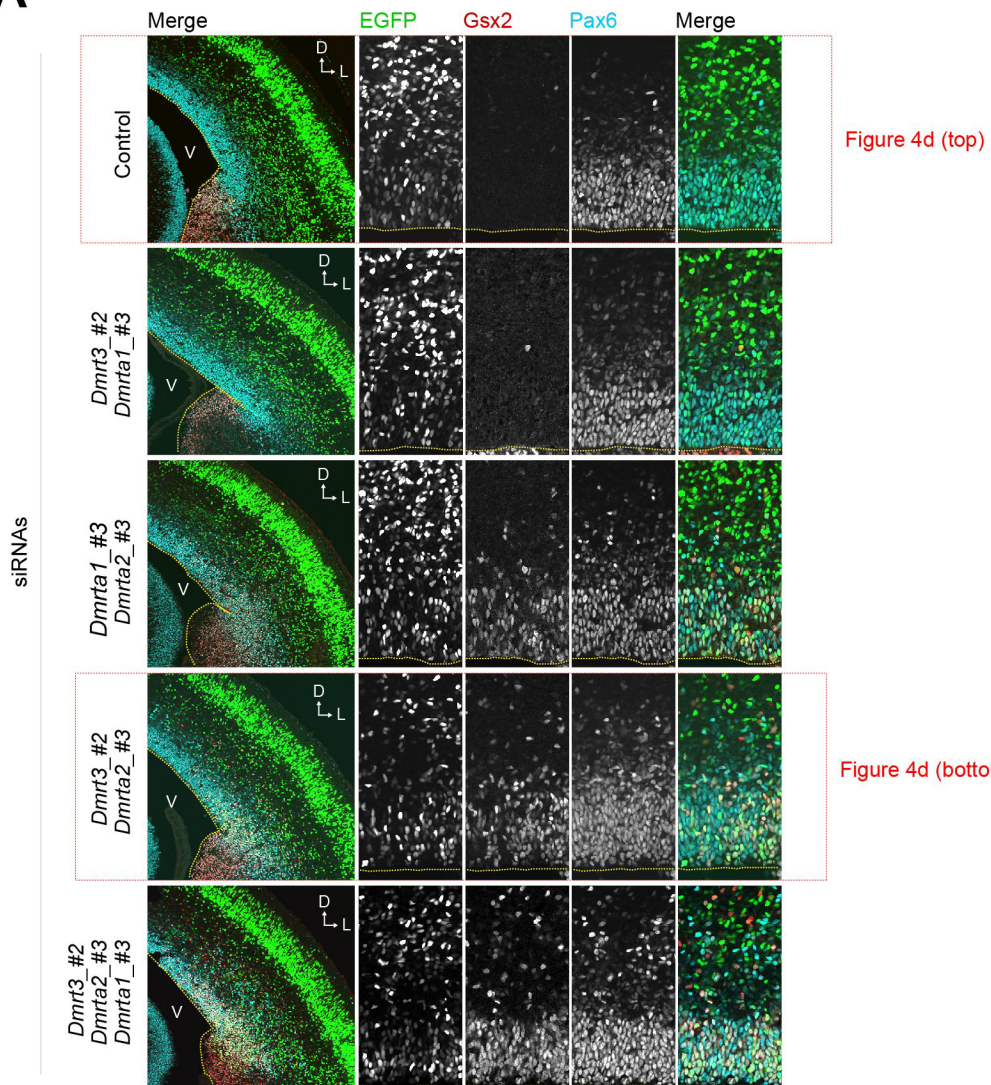
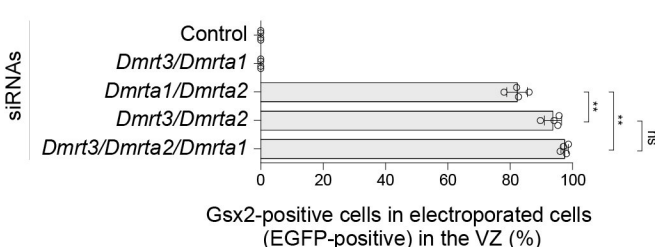
A**B**

Figure S6. Acute knockdown of *Dmrt* genes phenocopies *Dmrt3* and *Dmrt2* double mutants.

A, Immunofluorescence for Gsx2 and Pax6, as well as EGFP fluorescence, in coronal sections of an E15.5 mouse telencephalon electroporated with the indicated combinations of siRNAs targeting *Dmrt3*, *Dmrt1*, and *Dmrt2*. **B**, The quantification of Gsx2-positive cells that emerged ectopically in the dorsal telencephalon following the knockdown of *Dmrt* genes. All of the error bars represent \pm s.d. ($n=4$ per group). The statistical significance was determined using Student's *t*-test with Welch's correction (ns, not significant; ** $p<0.01$).

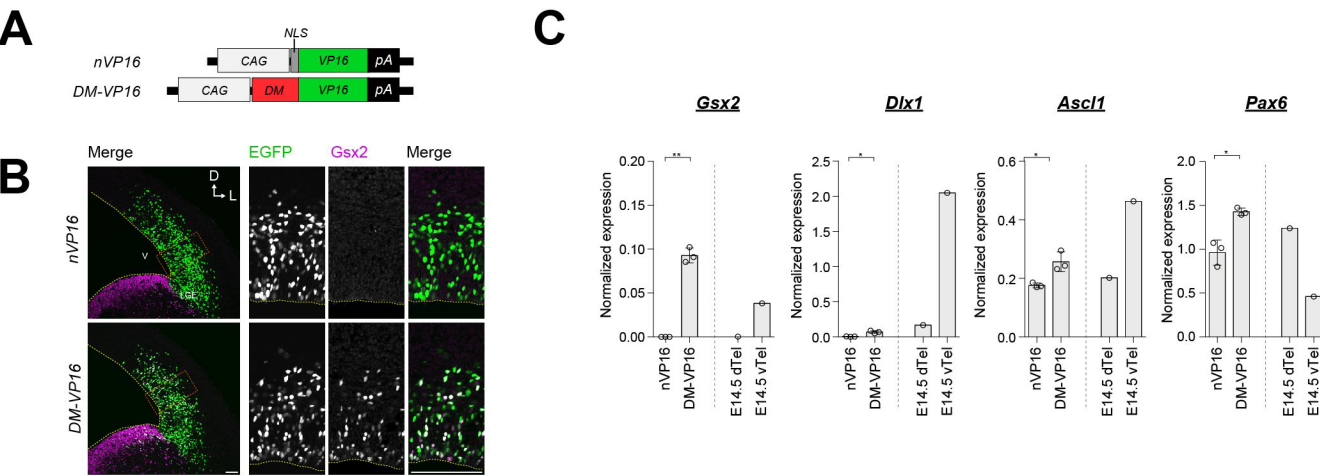


Figure S7. Overexpression of the VP16-fused DM domain in the dorsal telencephalon induces ectopic expression of Gsx2.

A, Structure of the expression plasmid for overexpressing the DM domain of Dmrt3 fused to the VP16 transactivation domain under the control the *CAG* promoter. Nuclear localization signal (NLS) fused to VP16 was used as control. **B**, Immunofluorescence for Gsx2, as well as EGFP fluorescence, in coronal sections of an E13.5 mouse telencephalon electroporated with the expression plasmid indicated in (A) at E12.5. **C**, Gene expression of *Gsx2*, *Dlx1*, *Ascl1*, and *Pax6* normalized to *Sox2* in the nVP16- (lane 1) and DM-VP16-transfected cells (lane 2), as determined using qPCR. All of the error bars represent \pm s.d. ($n=3$ per group). The statistical significance was determined using Student's *t*-test with Welch's correction ($*p<0.05$; $**p<0.01$).

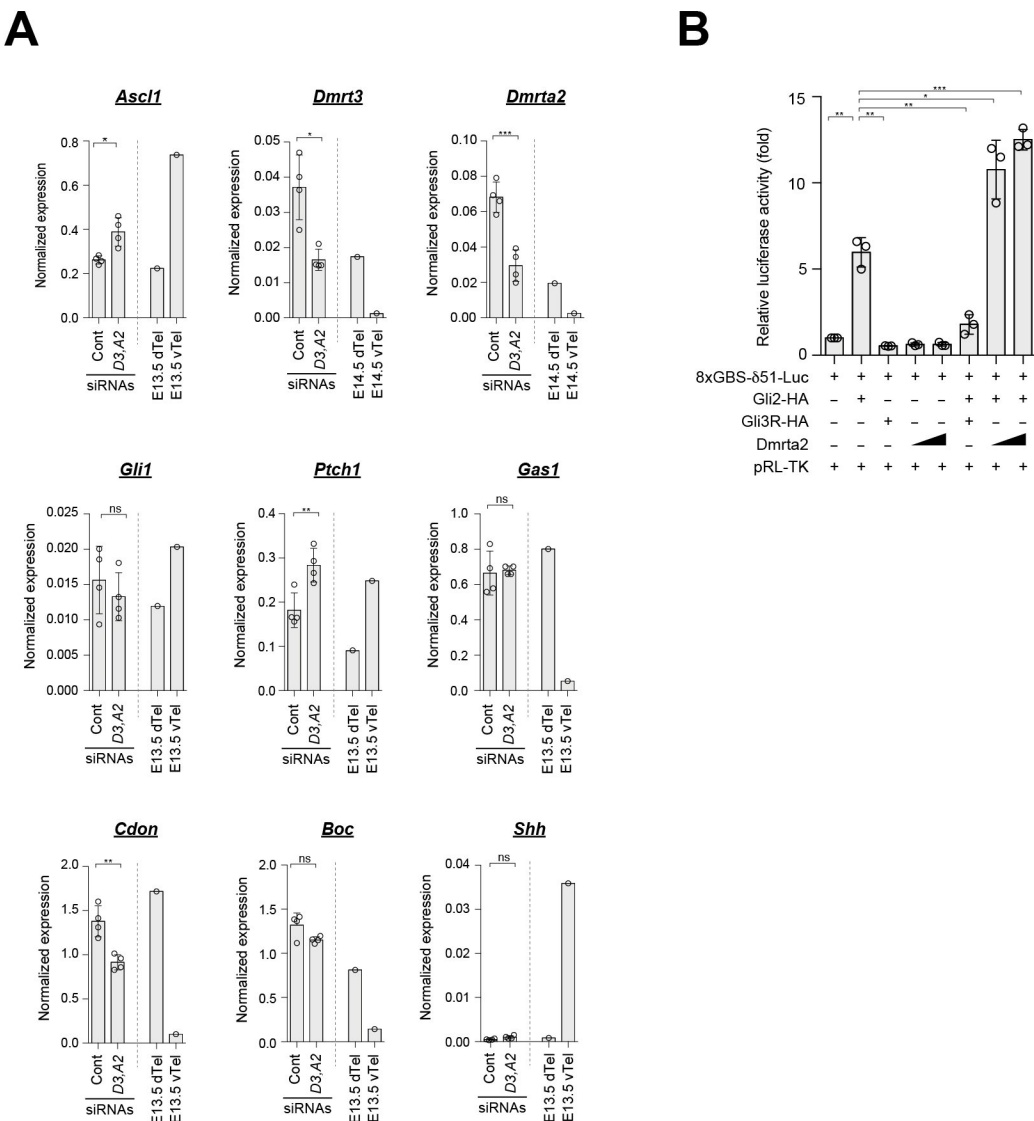
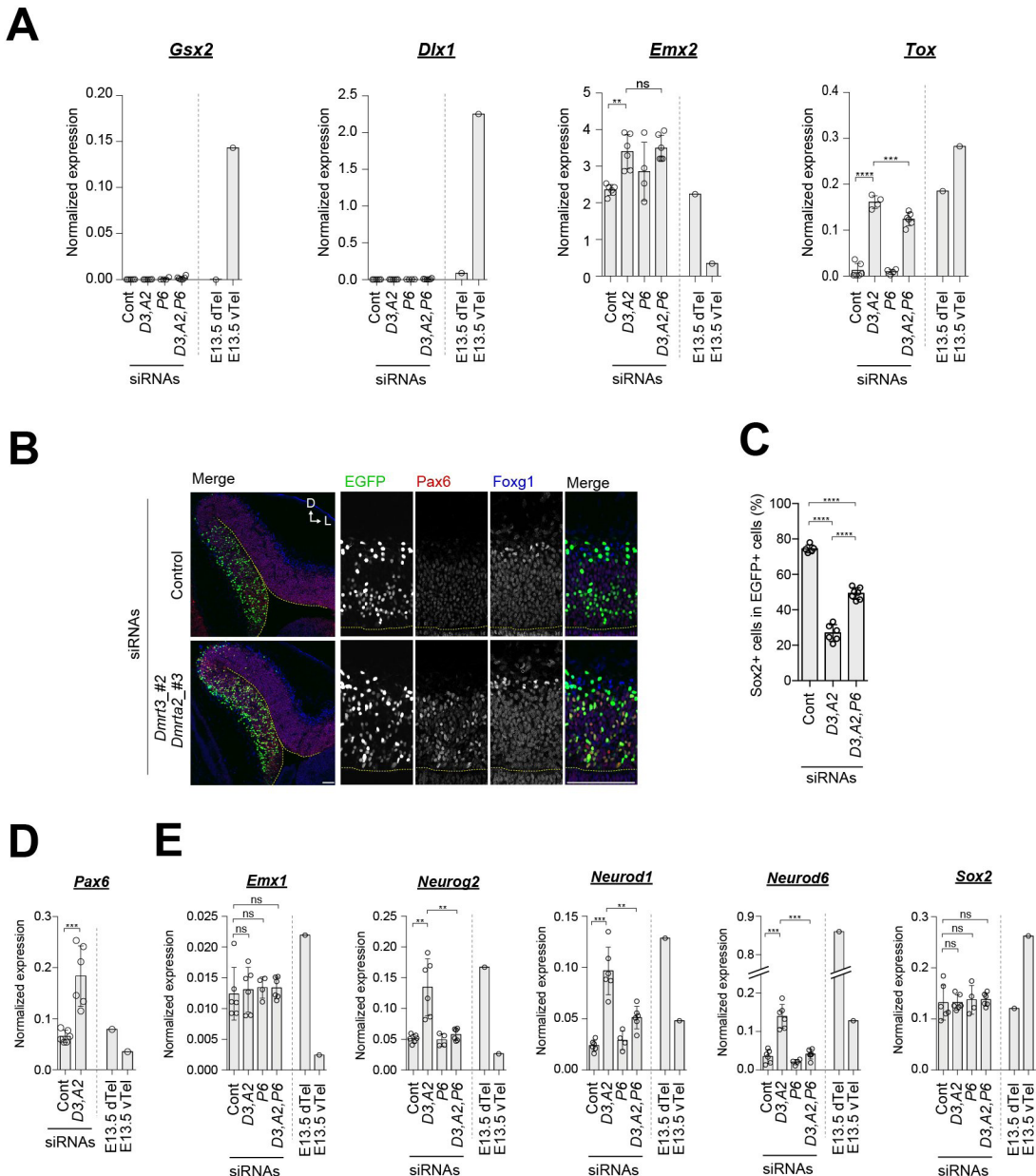


Figure S8. Dmrt factors do not affect the Shh signaling pathway.

A, Expression of Shh-signaling related genes, including *Ascl1*, *Dmrt3*, *Dmrt4*, *Gli1*, *Ptch1*, *Gas1*, *Cdon*, *Boc*, and *Shh* normalized to *Sox2* in control (lane 1) or double knockdown (*D3*, *A2*; lane2) cells, as determined using qPCR. The error bars represent \pm s.d. ($n=4$ per group).

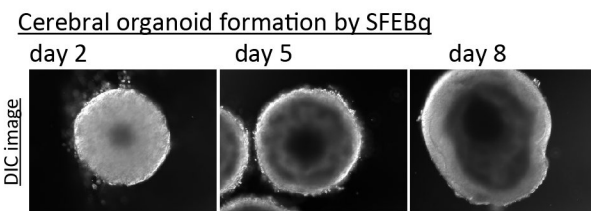
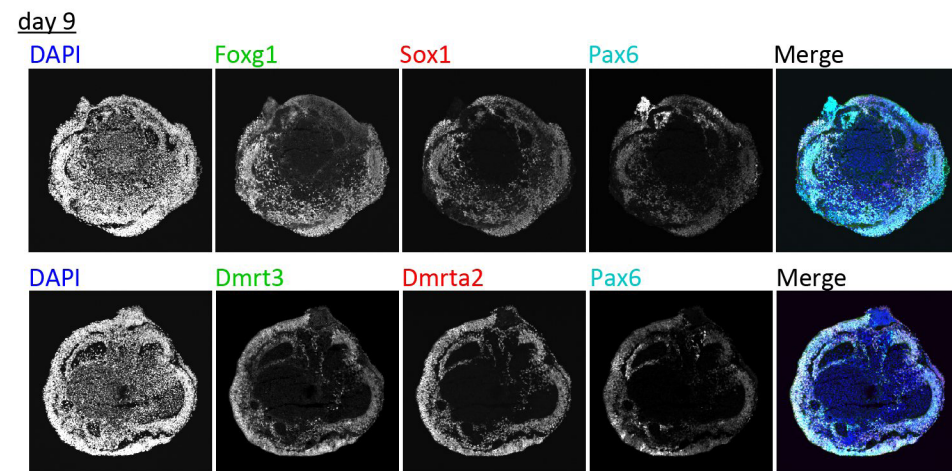
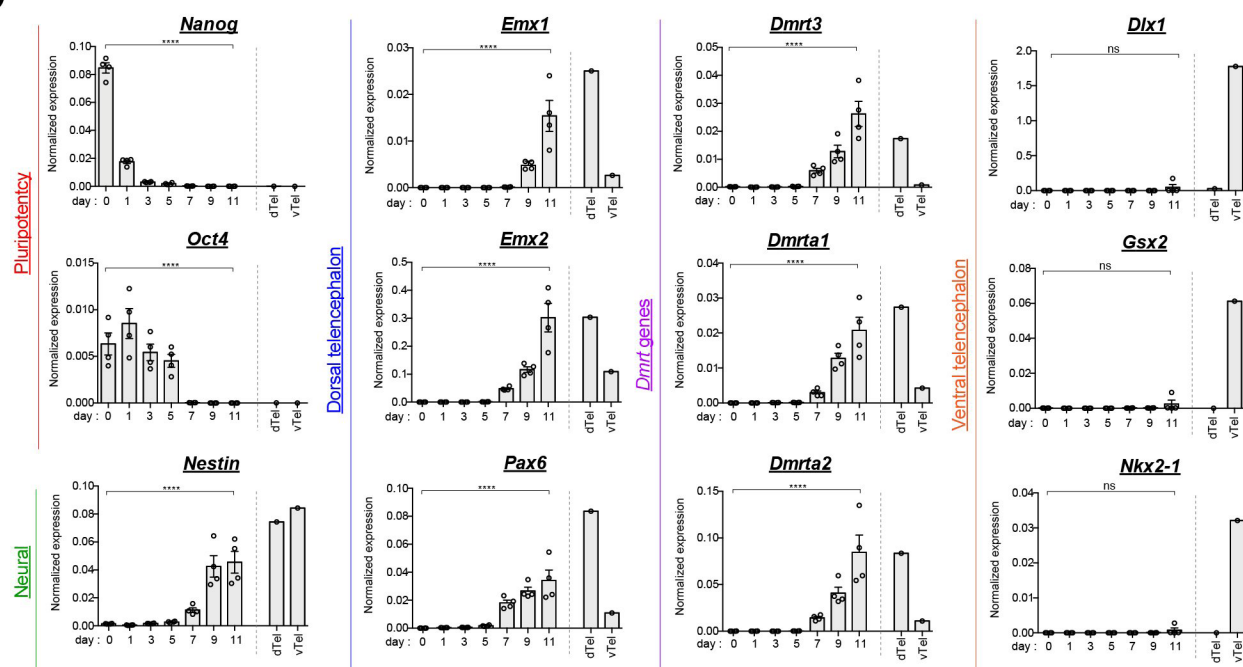
B, Influence of Dmrt expression on the transcriptional activation or repression of an 8 \times Gli binding sequence (8xGBS- δ S1-Luc) by Gli2 or Gli3R (a repressor form of Gli3). The error bars represent \pm s.e.m. ($n=4$ per group).

The statistical significance was determined using Student's *t*-test with Welch's correction (ns, not significant; **p*<0.05; ***p*<0.01; ****p*<0.001).

**Figure S9. Genetic interaction between *Dmrt* factor genes and *Pax6*.**

A, Gene expression of *Gsx2*, *Dlx1*, *Emx2*, and *Tox* normalized to *Sox2* in the electroporated cells, as determined by qPCR. The error bars represent \pm s.d. ($n=6$ per group). **B**, Immunofluorescence for *Pax6* and *Foxg1*, as well as EGFP fluorescence, in coronal sections of an E13.5 mouse telencephalon electroporated with control siRNAs or siRNAs targeting *Dmrt3* and *Dmrt2*. **C**, The quantification of *Sox2*-positive neural progenitors in the electroporated cells at E13.5. The error bars represent \pm s.d. { $n=5$ (cont), $n=6$ (*D3,A2*), $n=7$ (*D3,A2, Pax6*)}. **D**, **E**, Gene expression of *Pax6* (D), *Emx1* (E), *Neurog2* (E), *Neurod1* (E) and *Neurod6* (E) normalized to *Gapdh* in the electroporated cells, as analyzed by qPCR. The error bars represent \pm s.d. { $n=6$ per group in (E), $n=6$ per group in (F)}.

The statistical significance in (A), (C), (D), and (E) was determined using Student's *t*-test with Welch's correction (ns, not significant; ** $p<0.01$; *** $p<0.001$; **** $p<0.0001$).

A**B****C****Figure S10. Formation of cerebral organoids from mouse ES cells.**

A, DIC images of cell aggregates established using SFEBq-mediated formation of cerebral organoids on day 2, 5, and 8. **B**, Immunofluorescence for Foxg1, Sox1, Pax6, Dmrt3, and Dmrt2 in cerebral organoids on day 9. **C**, Gene expression of marker genes for pluripotency (*Nanog* and *Oct4*), neural fate (*Nestin*), dorsal telencephalic fate (*Emx1*, *Emx2*, and *Pax6*), the *Dmrt-A* gene family (*Dmrt3*, *Dmrt1*, and *Dmrt2*), and the ventral telencephalic fate (*Dlx1*, *Gsx2*, and *Nkx2-1*) normalized to *Gapdh*. The error bars represent ±s.e.m. (n=4 per group). The statistical significance was determined using one-way ANOVA (ns, not significant; ****p<0.0001).

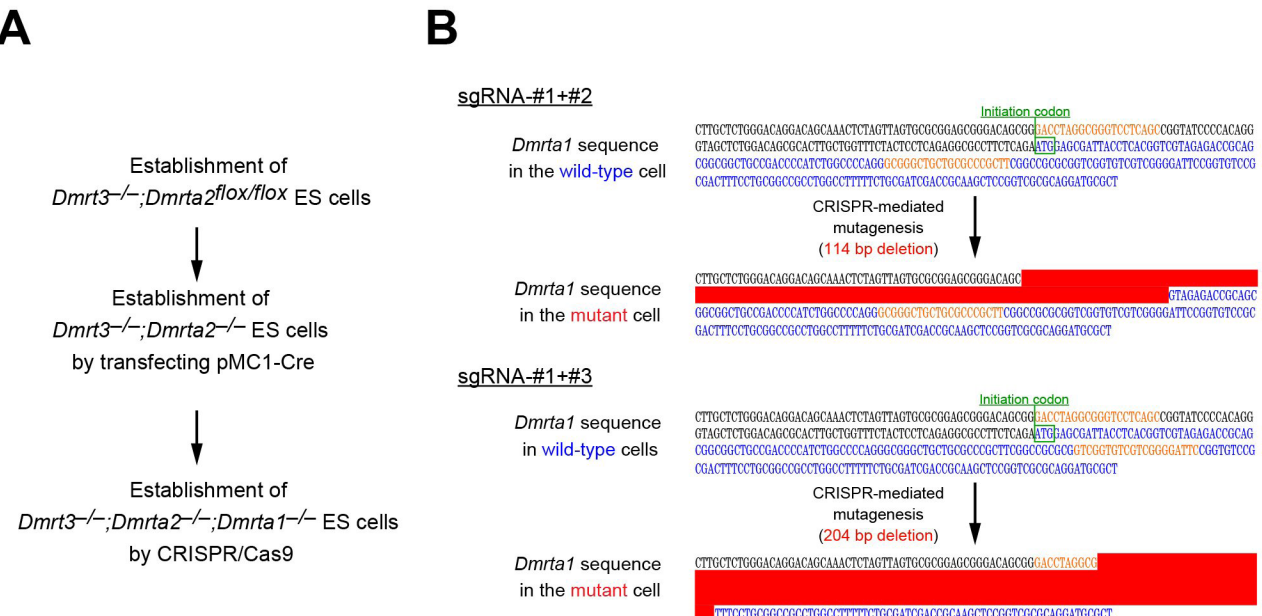


Figure S11. Establishment of the *Dmrt3*/*Dmrt2*/*Dmrt1*-mutant ES cells.

A, Schematic summarizing the establishment of the *Dmrt*-mutant ES cells. The *Dmrt3*^{-/-};*Dmrt2*^{flox/flox} ES cells were prepared first, and the *Dmrt2* gene was deleted subsequently to isolate *Dmrt3*/*Dmrt2* mutant ES cells by transfecting with an expression plasmid encoding Cre recombinase. The *Dmrt3*, *Dmrt1*, and *Dmrt2* triple knockout ES cells were established using *Dmrt3*/*Dmrt2* DKO ES cells by transfecting CRISPR/Cas9 plasmids targeting *Dmrt1*. **B**, Confirmation of successful CRISPR/Cas9-mediated deletion of the genomic sequence near the *Dmrt1* start codon in *Dmrt3*/*Dmrt2* DKO ES cells. Two sets of guide RNA sequences were used independently to establish the mutant cells. The DNA sequences indicated in blue and orange represent the open reading frame (ORF) of *Dmrt1* and the CRISPR/Cas9 target sequences, respectively.

Table S1Primers for RT-qPCR

Gene	Forward (5'-3')	Reverse (5'-3')	Reference
Gapdh	TGACCACAGTCATGCCAT	GACGGCACATTGGGGTAG	Kamiya et. al., 2011
Sox2	CATGAGAGCAAGTACTGGAAG	CCAAGGATATCAACCTGCATGG	Kawaguchi et. al., 2008
Nestin	CTCCTGGAACCTGTTCA	AGTGCTCAGTCCAGCTTC	Primer-BLAST
Tox	CACAAGTTGCAACCAAGCG	TACAGCGCTTGTCCCTG	Primer-BLAST
Pax6	GGAGAGAGCATGATCGAG	TGAAGTGCTTAACCGCCA	Primer-BLAST
Neurog2	GTCAAAGAGGACTATGGCGTGT	TACAGTCTTACGAGGTTCCCCACG	Kawaguchi et. al., 2008
Ascl1	GCCTCCATTGAAAGCAAGTC	AGAAGCAAAGACCGTGGGAG	Primer-BLAST
Gsx2	GACCCACGGAGATTCAC	CGCTGTCCATCCTTTGC	Primer-BLAST
Nkx2-1	TTCTGAAGCCGAATATCCA	ACGGAGTCGTGTTGG	Tucker et. al., 2008
Dlx1	TCCGAGAAGAGTACGGTGGT	ACTTGAGGCTTGTCTGG	Lo Iacono et. al., 2008
Neurog2	GTCAAAGAGGACTATGGCGTGT	TACAGTCTTACGAGGTTCCCCACG	Kawaguchi et. al., 2008
Neurod1	ACAGACGCTCTGAAAGTTT	GGACTGGTAGGAGTAGGGATG	Primer-BLAST
Neurod6	CACGGTGTCCAAAATATGC	GAATGTGGAGTAGGGTGCCT	Primer-BLAST
Fgf3	AAGCCAGCAGCTGCACACA	TCAAACGGCACGGAGGTCCA	Boroviak et. al., 2014
Dmrt3	TGCAACCGACTATGAGCAGGGA	TGTCTCTGAAAAGGCCGAGC	Kawaguchi et. al., 2016
Dmrt1	ACTGGTCCAGCATGCC	GGACGGCTCCATAATCATCC	Primer-BLAST
Dmrt2	CGTTCGGTATTCGTC	ACTCACACTGCACCAAGGAA	Primer-BLAST
Dmrt3 (detecting knockdown)	CTACGCCCTCGCAGTC	CGCAGTGTGTCGTTGAAAC	Primer-BLAST
Dmrt2 (detecting knockdown)	CGGCCCTGCTACGAACT	TCGGGCACAAAGGCTTC	Primer-BLAST
Gas1	CCTCTGACCCACGTCTTA	CCTAGATGGCAGTACCGAGC	Primer-BLAST
Cdon	GTCGGAATTGCCGAAACAC	GGGGCTTCATTTCCAGACCA	Primer-BLAST
Boc	GATTGAAGTAGACGAGGGAAAC	GATGGCATGATCAGGTAGTTGT	Lee et. al., 2010
Gli1	CCAAGCACCAGAACCGGACC	ACTGCTTCAGTGTGTTGCG	Primer-BLAST
Ptch1	CTATCCATCAGCGTGTGCT	AATAGAGGCCCATCATGCCA	Primer-BLAST
Emx1	ATATCAACGGTGGCCATC	GCCCTTGTTGCTCTTGATT	Primer-BLAST
Emx2	ATTGCTACCAAGCAGGCGAG	TCTTGCTCTGTGCTGTCATT	Primer-BLAST
mKO2	CTCCGTCATGGCATGAGT	GCGCAGTGTATCCTGT	Primer-BLAST
NesE-TetON-A2	TACGCCCTCAGCGACCTCAT	AGATCCGGTGGATCCCAC	Primer-BLAST

Primers for ChIP-qPCR

Target gene	Forward (5'-3')	Reverse (5'-3')	Reference
Pax6-A	CAGAGCGGGTTAGAGAAGG	GAGCCACAGGATTCCCA	Primer-BLAST
Pax6-B	ATGGGAACAATCCTGCGCT	GTCTCTTCAGCTAGACGCT	Primer-BLAST
Pax6-C	TATGTTCTTAACCTGTTCTGTTG	AAGCCCCAGCACCTACCTGTGCATACC	Primer-BLAST
Pax6-D	AGGCTGGTTACTTATTGCTCTGACAC	TCATTAGATTATACTGGTGGCAGAGAC	Primer-BLAST
Gsx2-A	TGTACAGTAATTACACGCTTGTACTG	AGGGTCCCTGTTAGGGATATTTAAC	Primer-BLAST
Gsx2-B	ACTTTAACAGGCTCACATGCGATG	TGCTAATGGCTGGAATATAGTTAGAATTG	Primer-BLAST
Gsx2-C	CTGGAGGGAGACGCGTTAG	TCCTCCCTTTCAGCTTGCC	Primer-BLAST
Gsx2-D	CCTGCCAATCAACCAAGGG	AGTTCTCAGCACTTGCC	Primer-BLAST